Presented at the 24th European Photovoltaic Solar Energy Conference and Exhibition, Hamburg, Germany, 21-25 Sep. 2009

BAND-GAP-ENGINEERED ARCHITECTURES FOR HIGH-EFFICIENCY MULTIJUNCTION CONCENTRATOR SOLAR CELLS

R. R. King, A. Boca, W. Hong, X.-Q. Liu, D. Bhusari, D. Larrabee, K. M. Edmondson,
D. C. Law, C. M. Fetzer, S. Mesropian, and N. H. Karam
Spectrolab, Inc., 12500 Gladstone Ave., Sylmar, CA 91342 USA

ABSTRACT: Beginning with maximum theoretical efficiencies from detailed balance calculations, we evaluate the real-world energy loss mechanisms in a variety of high-efficiency multijunction cell architectures such as inverted metamorphic 3- and 4-junction cells, as a step toward closing the gap between theory and experiment. Experimental results are given on band-gap-engineered lattice-matched and metamorphic 3-junction cells, and on 4-junction terrestrial concentrator cells. A new world record 41.6%-efficient solar cell is presented, the highest efficiency yet demonstrated for any type of solar cell.
Keywords: III-V Semiconductors, Concentrator Cells, High-Efficiency, Multijunction Solar Cell, Gallium Arsenide Based Cells, Lattice-Mismatched, Metamorphic

1 INTRODUCTION

Multijunction solar cells for concentrator photovoltaic (CPV) systems can have over 70% theoretical efficiency. The key question for terrestrial electricity generation, however, is "how much of this efficiency potential can be realized in practical solar cells and converted to kilowatt-hours at the electric meter?"

Experimental III-V multijunction solar cells have demonstrated efficiencies over 40% since 2006 [1], and are the highest efficiency PV technology known presently. But various mechanisms analyzed below still result in a chasm between the efficiencies promised from theoretical calculations, and those reached in practice.

Beginning with maximum theoretical efficiencies from detailed balance calculations, we evaluate the real-world energy loss mechanisms in a variety of high-efficiency multijunction cell architectures such as inverted metamorphic 3- and 4-junction cells, as a step toward closing the gap between theory and experiment. Experimental results are given on band-gap-engineered lattice-matched and metamorphic 3-junction cells, and on 4-junction terrestrial concentrator cells. A new world record 41.6%-efficient solar cell is presented, the highest efficiency yet demonstrated for any type of solar cell. This experimental Spectrolab concentrator cell, with a III-V lattice-matched 3-junction design and reduced metal coverage fraction, has been independently verified at NREL under standard test conditions (25°C, AM1.5D, ASTM G173-03 spectrum), at 364 suns (36.4 W/cm^2).

2 HIGH-EFFICIENCY CELL ARCHITECTURES

The main candidates for new high-efficiency multijunction cell designs draw on the principles of finding semiconductor band gaps that are more suited for conversion of the solar spectrum, *e.g.*, metamorphic materials and Al- or N-containing compounds; dividing the solar spectrum more finely through the use of multiple subcells; and driving the cell farther out of equilibrium through the use of high incident light intensity (higher concentration ratios).

Figures 1-4 show cell schematics, concepts, and corresponding modeled subcell and multijunction cell light I-V characteristics, for four of these candidate architectures for high-efficiency multijunction (MJ) terrestrial concentrator cells. The upright metamorphic

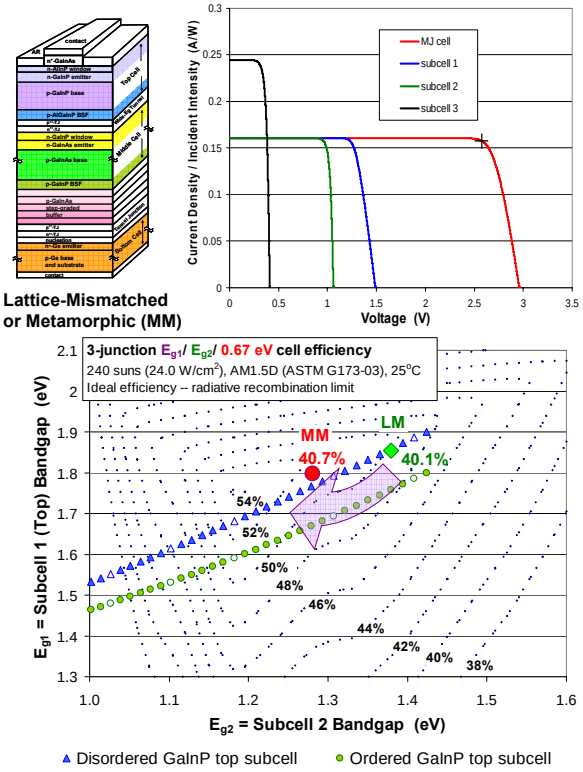

Figure 1. Cross-sectional diagram, modeled I-V curves and iso-efficiency contour plot for upright metamorphic (MM) 3-junction cell architecture.

(MM) 3-junction design [2-5] in Fig. 1, *e.g.*, the 1.78/ 1.30/ 0.67 eV cell modeled in the I-V chart, uses metamorphic GaInP and GaInAs to lower the band gaps of the upper two subcells to a more advantageous theoretical combination, as shown by the arrow in the contour plot of cell efficiency. The inverted metamorphic (IMM) 3-junction [6-8] design in Fig. 2, *e.g.*, the 1.90/ 1.40/ 1.00 eV cell of the I-V chart, instead raises the band gap of the third and bottommost subcell, through the use of MM materials. The arrow in the contour plot of theoretical efficiency vs. subcell 2 and subcell 3 band gaps again indicates the shift toward more optimum band gaps for solar conversion. The general 4-junction cell architecture [9] shown in Fig. 3 may be

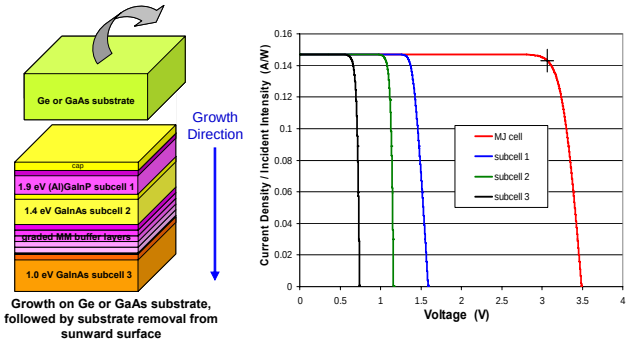

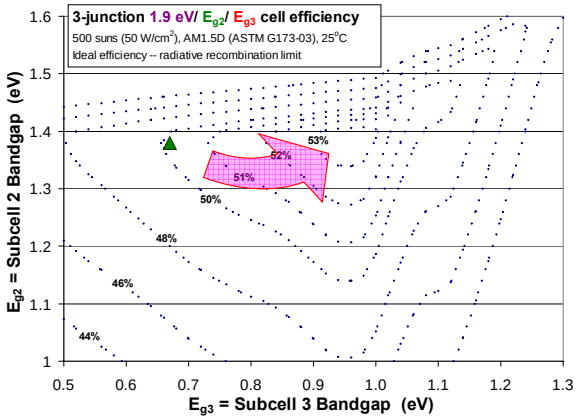

Figure 2. Schematic diagram, modeled I-V curves and iso-efficiency contour plot for inverted metamorphic (IMM) 3-junction cell architecture.

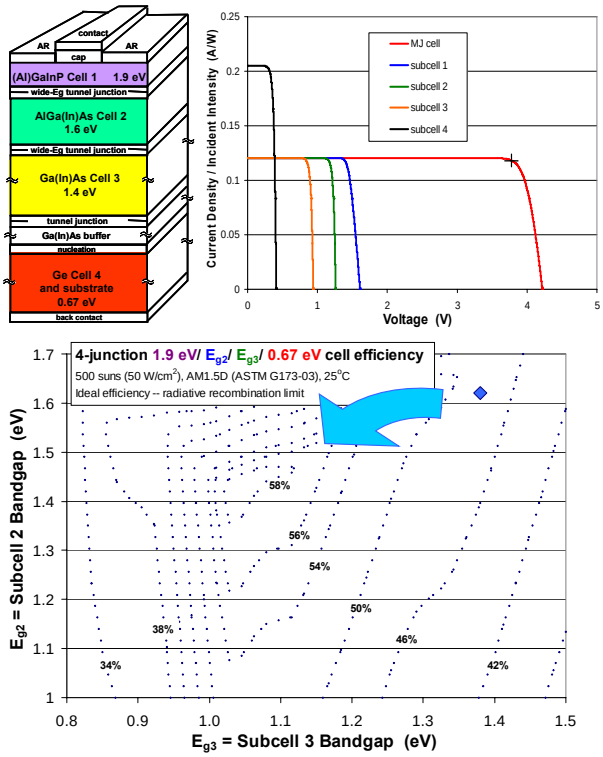

Figure 3. Schematic diagram, modeled I-V curves and iso-efficiency contour plot for 4-junction terrestrial in the concentrator cell architectures, which may have a lattice-matched (LM), upright metamorphic, inverted metamorphic, or wafer-bonded design.

of a lattice-matched (LM), upright metamorphic, inverted metamorphic, or wafer-bonded design. This type of cell trades off current for increased voltage, as shown in the modeled I-V chart for a metamorphic 1.90/ 1.55/ 1.20/ 0.67 eV 4-junction cell, giving lower I^2R series resistance losses, and the efficiency can be substantially raised by adjusting the subcell 2 and 3 band gaps, as shown in the contour plot. An upright metamorphic 4-junction cell with this subcell band gap combination is shown in Fig. 4. The 4-junction design can be extended to 5, 6 or more junctions, as in the 5-junction inverted metamorphic cell shown in schematic in Fig. 5a, and the 5-junction cell in Fig. 5b in which the desired band gaps are achieved by semiconductor-to-semiconductor bonding, or wafer bonding, subcells grown on different substrates. Finally, Fig. 6 shows a cell schematic, modeled I-V curves, and spectrum partition for a more radical 6-junction terrestrial concentrator cell architecture [9], with band gaps of 2.00/ 1.78/ 1.50/ 1.22/ 0.98/ 0.67 eV.

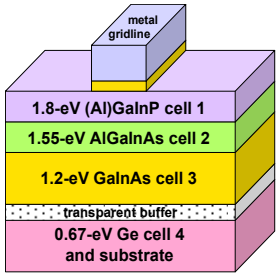

Figure 4. Schematic diagram of a 4-junction upright metamorphic solar cell.

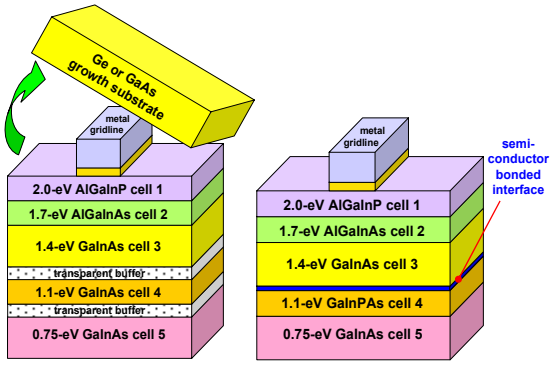

Figure 5. Schematic diagrams of high-efficiency terrestrial concentrator solar cells with (a) a 5-junction inverted metamorphic cell structure, and (b) a 5-junction wafer-bonded cell structure in which the desired band gaps are achieved by semiconductor-to-semiconductor bonding subcells grown on different substrates.

Cell designs with high theoretical efficiency often call for band gaps that are a challenge to reach in high quality semiconductor materials on conventional substrates, *e.g.*, semiconductors with >2.0 eV and those ~1 eV at the Ge lattice constant. The main next-generation terrestrial CPV cell candidates – such as upright and inverted metamorphic cells, cells with 4, 5, and 6 junctions, and multijunction cells formed by wafer-bonding subcells with different lattice constants grown on two or more substrates – each represent a different

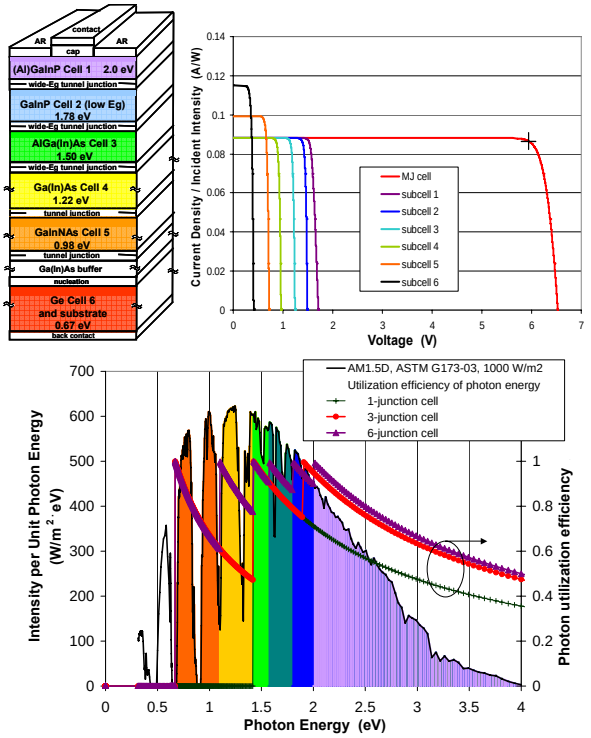

Figure 6. Schematic diagram, modeled I-V curves and partition of the solar spectrum for a 6-junction terrestrial concentrator cell design with low series resistance losses and very high efficiency.

approach toward the same goal of reaching the most advantageous subcell band gaps for energy conversion in a multijunction cell. Adding more subcells in a multijunction stack increases efficiency by partitioning the solar spectrum into smaller slices, but also increases sensitivity to the non-ideal properties of tunnel junctions, and current matching among subcells. Higher concentration brings the available voltage at the cell terminals closer to the maximum allowed by the band gap, but also increases series resistance power loss, and adds to the cost of the concentrating optics. Further real-world issues include the cost and manufacturing robustness of some new high-efficiency cell designs, and the actual energy harvested by solar cells with 3, 4, 5, and 6 junctions, considering the current match among subcells with varying solar spectrum over the course of the day and year [9].

3 MULTIJUNCTION CELL MODELING

Differences between solar cell maximum theoretical performance limits and experimental efficiencies are investigated below, in order to guide research to identify and minimize the gap between the two. The maximum efficiency allowed by the second law of thermodynamics for a multijunction cell can be determined by finding the photogenerated current density J_{ph} in each subcell, and applying the principle of detailed balance [10] to calculate the diode saturation current density J_o of each subcell. This upper limit on efficiency is calculated for 3- and 4-junction metamorphic solar cells as a function of incident intensity in Fig. 7, using the expression for J_o in Eq. 1, calculated from detailed balance [10-13].

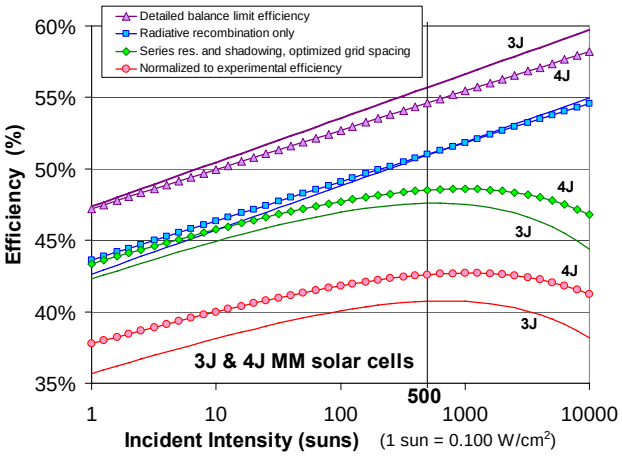

Figure 7. Calculated efficiency of 3J and 4J metamorphic solar cells using successively more realistic models: 1) detailed balance; 2) radiative recombination only; 3) series resistance and grid shadowing; and 4) normalization to experimental 3J cell efficiency.

$$J_o = \frac{2\pi kTq}{h^3c^2}\left(E_g + kT\right)^2 e^{-E_g/kT} \qquad (1)$$

In this physical model, not only are non-ideal recombination mechanisms like Shockley-Read-Hall (SRH) recombination assumed to be zero, but even the fundamental recombination mechanism of radiative recombination is suppressed, and the only emission escaping the solar cell is that due to thermal radiation, treating the solar cell as a non-ideal blackbody at the cell temperature, that emits only in the wavelength range where the solar cell also absorbs light, *i.e.*, for photon energies greater than the solar cell band gap [10]. For solar cells with direct band gap semiconductors, as in III-V multijunction cells, the actual emission spectrum is quite different, consisting mainly of photon emission from radiative recombination at the band gap energy of each subcell. One interpretation for this difference is that if photon recycling, in which photons emitted by the radiative recombination process are reabsorbed to create an electron-hole pair elsewhere in the semiconductor, were to capture the photon from nearly every electron-hole recombination event, the radiative recombination emission spectrum would be suppressed leaving only the non-ideal blackbody spectrum of the detailed balance model [14].

In a sequence of increasingly realistic physical models, the case in which radiative recombination – the inverse of the essential process of photogeneration of electron-hole pairs in a solar cell – is considered to be the only recombination mechanism is treated next in Fig. 7. At 500 suns for example, the calculated efficiency of the 4J MM cell considered here goes from 55% in the detailed balance model, to 51% in the radiative recombination model, in which none of the emission from radiative recombination is assumed to be recaptured by photon recycling.

Next, the losses associated with the series resistance and shadowing of the metal grid on the multijunction cell are calculated in Fig. 7, assuming a technologically relevant metal grid width of 6 μm, and with the grid

spacing reoptimized at each concentration level. Although the 3J cell has had similar or even higher calculated efficiency up to this point, the advantage of lower current density in the 4J cell begins to show in the series resistance and shadowing calculations in Fig. 7; at 500 suns the 4J cell design is ~48.5%, with the 3J cells nearly 1% lower in absolute efficiency. The difference between 4J and 3J cells becomes more pronounced for even higher concentrations.

Finally, the lowest set of curves in Fig. 7 show the predicted efficiency when normalization factors for V_{oc}, J_{sc}, and FF observed on experimental 3J cells are applied to the calculated efficiency. These curves normalized to experimental efficiency should give the closest correspondence to actual cell efficiency. At 500 suns for the specific band gap combinations considered in Fig. 7 (1.90/ 1.64/ 1.30/ 0.67 eV for 4J and 1.78/ 1.30/ 0.67 for 3J), the calculated efficiency normalized to experimental cell efficiency is ~43% for 4J cells, compared to ~41% for 3J cells. Note that although 3J cells are calculated to have similar or higher performance compared to 4J cells for the ideal efficiency cases of detailed balance and radiative recombination only, the high-voltage, low-current design of 4J cells gives them a significant efficiency advantage at 500 suns and above for the more realistic cases where series resistance, grid shadowing, and normalization to experimental cell values are taken into account. An important question, requiring both modeling and field testing to answer, is how solar cells with 4 (or more) junctions will fare compared to 3J cells under the real solar spectrum which changes as a function of sun angle and meteorological conditions [9].

The difference between each of the physical models treated in Fig. 7 presents an opportunity for bringing the performance of actual multijunction cells closer to their theoretical potential. The difference between detailed-balance and radiative-recombination-only models might be bridged if photon recycling were made very efficient, such that nearly every photon from a radiative recombination event were reabsorbed to create an electron-hole pair elsewhere in the semiconductor. The cell performance change associated with grid series resistance and shadowing can be addressed through improved grid technology and through the use of high-voltage, low-current cell designs such as those with 4 or more junctions. Finally, the further difference with respect to the actual V_{oc}, J_{sc}, and FF of the best experimental cells can be addressed by device improvements such as semiconductor layers with higher bulk lifetime and better interface passivation to reduce SRH recombination, and more transparent, highly conductive tunnel junctions.

3 EXPERIMENTAL RESULTS

A new record efficiency for a photovoltaic cell has been achieved, with 41.6% efficiency measured under standard test conditions for concentrator cells (25°C, AM1.5D, ASTM G173-03 spectrum) at 364 suns (36.4 W/cm^2). This record efficiency cell, built at Spectrolab with a lattice-matched 3-junction structure and reduced grid coverage fraction, has the highest efficiency yet demonstrated for any type of solar cell. The 41.6% efficiency result was independently verified by measurements at the National Renewable Energy Laboratory (NREL). The light I-V characteristic of this cell is plotted in Fig. 8, showing measured parameters of V_{oc} = 3.192 V, J_{sc}/intensity = 0.1468 A/W, FF = 0.8874 , and efficiency = 41.6 % at 364 suns.

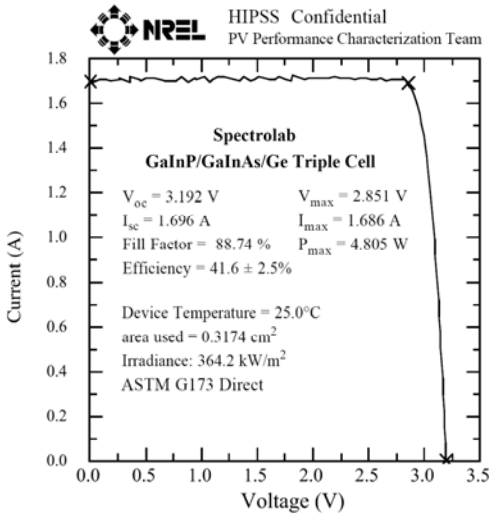

Figure 8. Light I-V characteristic for record efficiency 41.6%-efficiency concentrator solar cell, built at Spectrolab with a lattice-matched 3-junction cell structure, and independently verified at NREL.

In Fig. 9, the efficiency, V_{oc}, and FF of this record cell are plotted with incident intensity varying from 0.9 to 940 suns. The efficiency peaks at 41.6% at 364 suns and drops for higher concentrations due to series resistance, but is still over 40% at 820 suns, and is 39.8% at 940 suns. The fill factor shows a broad plateau over ~2 decades in incident intensity, rising rapidly between 1 and ~4 suns due to increasing excess carrier concentration, and decreasing above ~400 suns due to series resistance. The V_{oc} increases at an average rate of ~80 mV per decade in incident intensity, per junction, in the intensity range from 1 to 10 suns. From 10 to 100 suns this rate is 75 mV per decade, while from 100 to 1000 suns it drops to 61 mV per decade. Thus over the 100 to 1000 sun range of interest, the average V_{oc} increase with concentration is fit fairly well by using diode ideality factor n = 1 for each of the 3 subcells.

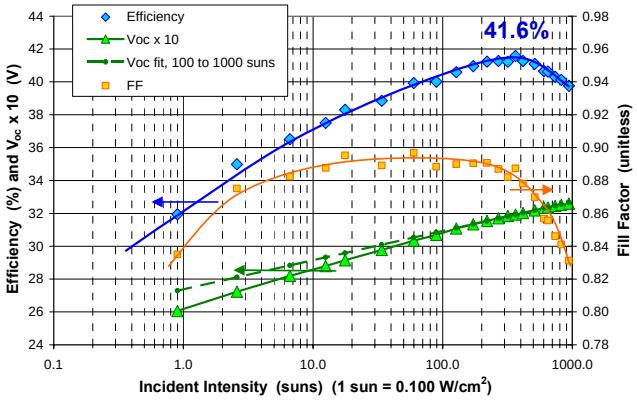

Figure 9. Measured light I-V parameters of the 41.6%-efficient solar cell as a function of incident intensity. The cell is still over 40% efficient at 820 suns, and has 39.8% efficiency at 940 suns.

The light I-V characteristics of the 41.6%-efficient, GaInP/GaInAs/Ge 3-junction cell are shown in Fig. 10, for a range of incident intensities from 2.6 to 940 suns. The rise in open-circuit voltage with increased light intensity is evident. Beyond about 400 suns, the V_{oc} continues to increase, but the fill factor and V_{mp} are clearly degraded, due to series resistance.

Figure 11 is a chart of the best research cell efficiencies confirmed by the National Renewable Energy Laboratory, showing the most recent 41.6%-efficient 3-junction GaInP/GaInAs/Ge solar cell. It is interesting to note that not only do multijunction concentrator cells have by far the highest efficiency of any photovoltaic cell technology, they are currently enjoying a more rapid rate of increase than other technologies such as crystalline silicon, thin-film compound semiconductor cells such as CIGS and CdTe, and amorphous Si cells.

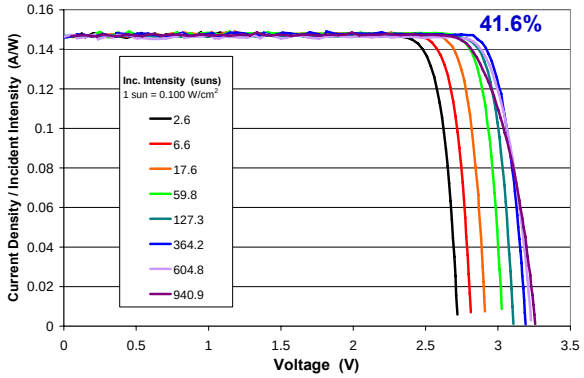

Figure 10. Series of light I-V curves measured over a range of incident intensities.

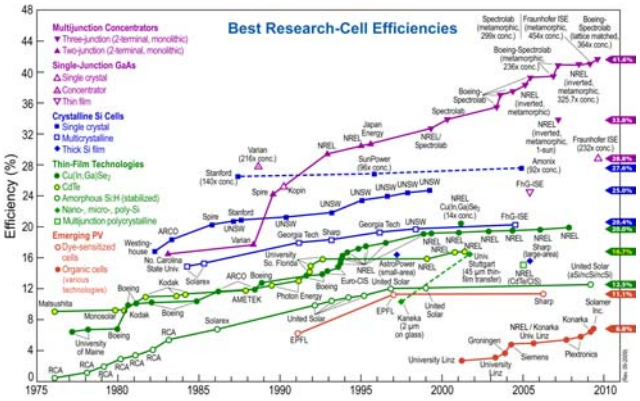

Figure 11. Chart of best research cell efficiencies for a variety of solar cell technologies, as confirmed by the National Renewable Energy Laboratory, showing the most recent 41.6%-efficient multijunction cell. Chart courtesy of Larry Kazmerski, NREL.

Many of the efficiency improvements of past experimental cells are beginning to impact production terrestrial concentrator cell efficiencies as well. The efficiency distributions of successive Spectrolab terrestrial concentrator solar cell product generations, the C1MJ, C2MJ, and most recent C3MJ cell products, are shown in Fig. 12. The cell distributions match well with the target average production efficiencies of these cell generations: 37.0%, 37.5%, and 38.5% efficiency at 500 suns (50.0 W/cm^2), AM1.5D, ASTM G173-03 spectrum, 25°C, respectively, for the C1MJ, C2MJ and C3MJ products. Additionally, although it is for a smaller sample size, the distribution of the C3MJ cell, Spectrolab's next concentrator cell product, is markedly narrower and sharper than earlier cell generations.

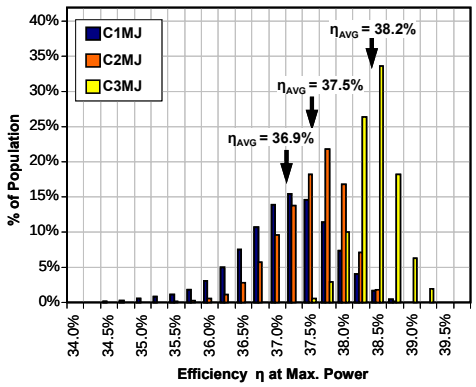

Figure 12. Cell efficiency distributions for successive Spectrolab terrestrial concentrator cell products, C1MJ, C2MJ, and C3MJ, with 37.0%, 37.5%, and 38.5% efficiency targets, respectively, at 500 suns.

Looking beyond the C3MJ production cell, the C4MJ cell has a 40% target average efficiency in production, and later concentrator cell products, C5MJ, C6MJ, and so on, are slated to have still higher production efficiencies. Fig. 13 shows preliminary data for a small number of experimental full-process 1-cm^2 cells with an upright metamorphic (MM) 3-junction cell structure, a candidate for the C4MJ cell. The light I-V data at 500 suns (50 W/cm^2), AM1.5D, ASTM G173-03, 25°C in Fig. 13 are corrected to correspond to standard calibration methods in production light I-V testing. These prototype cells with 5%-In GaInAs in the middle cell base include a variety of experiments in cell structure, not a frozen design, so the distribution width is expected to tighten markedly when the same cell structure is grown and processed day in and day out. Even so, the preliminary average efficiency measured for this experimental batch is 39.6%, and there are a substantial number of cells with efficiency above the 40% target.

To reach the ever higher efficiencies of future cell generations, the advanced cell architectures described in the first sections of the paper are being investigated. The performance of 4-junction terrestrial concentrator solar cells, one family of these advanced designs, is plotted in Figs. 14 and 15. Figure 14 shows the measured external quantum efficiency as a function of wavelength for the individual subcells in a lattice-matched 4-junction cell. The photogenerated current density J_{ph} in each subcell can be found by integrating with the standard AM1.5D (ASTM G173-03) solar spectrum, also plotted in Fig. 14. The current densities at one sun (0.100 W/cm^2) for this particular 4J cell are 9.0 mA/cm^2 for AlGaInP subcell 1, 8.8 for AlGaInAs subcell 2, 9.5 for GaInAs subcell 3, and 21.7 mA/cm^2 for Ge subcell 4. As seen in Fig. 14, opportunities for improving these concentrator 4J cells include increasing the quantum efficiency in the AlGaInP and AlGaInAs subcells 1 and 2 up to the ~90% level of

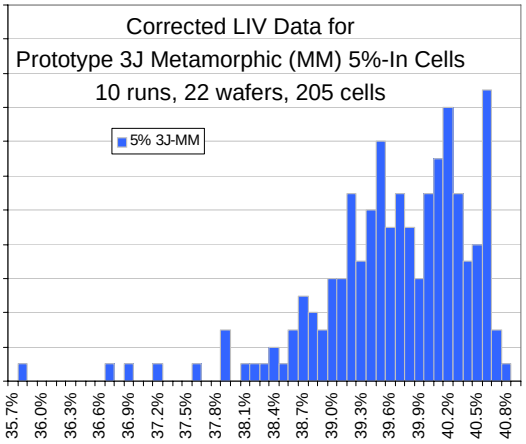

	Isc (A)	Voc (V)	FF	Eff
Average	7.601	3.090	0.845	39.6%
Std. dev.	0.135	0.022	0.009	0.8%

Figure 13. Efficiency distribution and average light I-V parameters for prototype full-process 1-cm^2-area metamorphic 3-junction cells, as described in the text.

the GaInAs subcell 3, improved current balance among the top 3 subcells, and use of metamorphic materials in 4J cells to achieve a better band-gap-engineered multijunction device structure as discussed above.

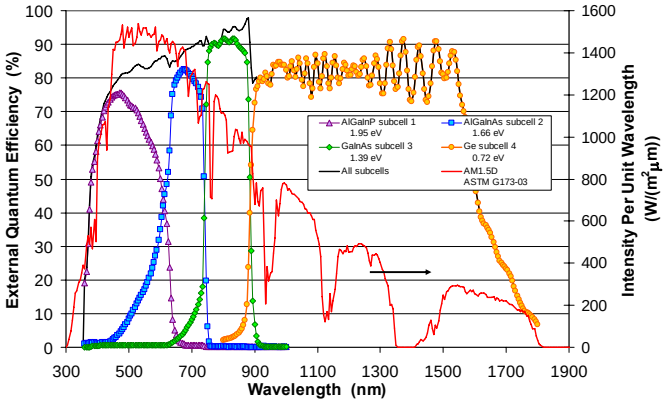

Figure 14. Measured external quantum efficiency for each of the 4 subcells in a lattice-matched 4-junction AlGaInP/ AlGaInAs/ GaInAs/ Ge terrestrial concentrator cell, along with the irradiance of the standard AM1.5D (ASTM G173-03) solar spectrum for comparison.

In Fig. 15, the illuminated I-V curve of a prototype 4-junction terrestrial concentrator cell is plotted, showing its high-voltage, low-current characteristics which lead to lower resistive power loss compared with 3-junction cells. These early prototype 4-junction concentrator cells have reached up to 36.9% efficiency at 500 suns (50 W/cm^2) at Spectrolab in unconfirmed measurements. The independently confirmed light I-V curves of the earlier record 40.7%-efficient metamorphic 3-junction cell [1], the present record 41.6%-efficient lattice-matched 3-junction cell at 364 suns, and the same cell measured to have 40.1% efficiency at 822 suns, are also plotted for comparison.

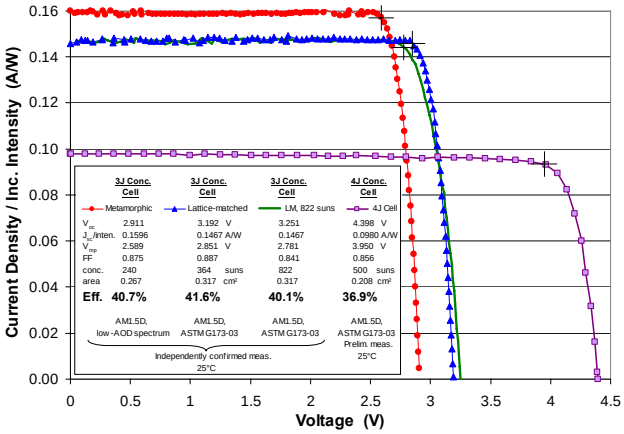

Figure 15. Light I-V measurements for a 4-junction terrestrial concentrator cell with 4.398 V open-circuit voltage and preliminary measured efficiency of 36.9% at 500 suns, compared with independently confirmed measurements on an earlier record 40.7% MM 3J cell [1], and the present record 41.6% LM 3J cell at 364 suns, measured to have 40.1% efficiency at 822 suns.

5 SUMMARY

The structures of several of the main candidate designs for next-generation 3- to 6-junction solar cells are described, and optimization of the subcell band gap combinations is discussed. Theoretical efficiency is calculated for terrestrial 3- and 4-junction concentrator solar cells as a function of incident intensity, beginning with the most idealized case of detailed balance efficiency, and progressing through a series of successively more realistic models, in order to identify theoretically allowed areas for further efficiency improvement. Experimental results are presented for present and future generations of production concentrator cells, for experimental 4-junction terrestrial concentrator cells, and for a new record 41.6%-efficient lattice-matched 3-junction cell, the highest efficiency yet demonstrated for any type of solar cell.

ACKNOWLEDGMENTS

The authors would like to thank Carl Osterwald, Keith Emery, Larry Kazmerski, Martha Symko-Davies, Fannie Posey-Eddy, Holly Thomas, Russ Jones, Jim Ermer, Peichen Pien, Dimitri Krut, Hector Cotal, Mark Osowski, Joe Boisvert, Geoff Kinsey, Kent Barbour, Mark Takahashi, and the entire multijunction solar cell team at Spectrolab. This work was supported in part by the U.S. Dept. of Energy through the NREL High-Performance Photovoltaics (HiPerf PV) program, the DOE Technology Pathways Partnership (TPP), and by Spectrolab.

REFERENCES

[1] R. R. King *et al.*, *Appl. Phys. Lett.*, **90**, 183516, 4 May 2007.
[2] R. R. King *et al.*, *Proc. 28th IEEE Photovoltaic Specialists Conf.* (2000), Anchorage, Alaska, p. 982.
[3] F. Dimroth, U. Schubert, and A.W. Bett, *IEEE Electron Device Lett.*, **21**, 209 (2000).

[4] T. Takamoto *et al.*, *Proc. 3rd World Conf. on Photovoltaic Energy Conversion* (2003), Osaka, Japan, p. 581.
[5] F. Dimroth *et al.*, *Proc. 34th IEEE Photovoltaic Specialists Conf.* (2009), Philadelphia, Pennsylvania.
[6] M. W. Wanlass *et al.*, *Proc. 31st IEEE Photovoltaic Specialists Conf.* (2005), p. 530.
[7] R. R. King *et al.*, *Proc. 20th European Photovoltaic Solar Energy Conf.* (2005), Barcelona, Spain, pp. 118-123.
[8] J. F. Geisz *et al.*, *Appl. Phys. Lett.*, **93**, 123505 (2008).
[9] R. R. King *et al.*, *Proc. 21st European Photovoltaic Solar Energy Conf.* (2006), Dresden, Germany, pp. 124-128.
[10] W. Shockley and H. J. Queisser, *J. Appl. Phys.*, **32**, 510 (1961).
[11] M. A. Green, *Third Generation Photovoltaics – Advanced Solar Energy Conversion*, Springer-Verlag, Berlin-Heidelberg (2003).
[12] J. Nelson, *The Physics of Solar Cells*, Imperial College Press, London (2003).
[13] S. Kurtz *et al.*, *Prog. Photovolt.: Res. Appl.*, **16**, 537 (2008).
[14] Personal communication, Richard M. Swanson, Sarah Kurtz.
[15] R. R. King *et al.*, *Proc. 23rd European Photovoltaic Solar Energy Conf.*, Valencia, Spain, Sep. 1-5, 2008.